Analyst

PAPER

View Article Online
View Journal | View Issue

Cite this: *Analyst*, 2014, **139**, 649

Fluorescent immunosensor based on CuS nanoparticles for sensitive detection of cancer biomarker†

Ying-Di Zhu,[a] Juan Peng,[b] Li-Ping Jiang*[a] and Jun-Jie Zhu[a]

Received 22nd October 2013
Accepted 6th November 2013

DOI: 10.1039/c3an01987j

www.rsc.org/analyst

A novel fluorescent immunosensor was developed based on the use of CuS nanoparticles (CuS NPs) as labels for the highly sensitive detection of human prostate cancer biomarker prostate specific antigen (PSA). In the presence of CuS NPs, the non-fluorescent substrate *o*-phenylenediamine could be oxidized into the stable fluorescent product 2,3-diamiophenazine at physiological pH. Throughout the reaction, no other oxidizing agents (*e.g.* hydrogen peroxide) were needed. The relatively mild oxidation conditions made the immunoassay robust, reliable and facile. The proposed immunoassay exhibited high sensitivity and specificity for the detection of PSA. A linear relationship between the fluorescent signals and the concentration of PSA was obtained in the range of 0.5 pg mL^{-1} to 50 ng mL^{-1}, with a detection limit of 0.1 pg mL^{-1} ($S/N = 3$). The proposed fluorescent immunoassay can be used as a promising platform for the detection of a variety of other biomarkers.

Introduction

Nowadays, the development of reliable and sensitive methods for the detection of cancer biomarkers plays an increasingly important role in the diagnosis and treatment of cancer.[1,2] Immunoassays have been the preferred methods for the selective and sensitive detection of various target biomarkers, especially proteins, based on the specific and strong recognition of antibodies to their corresponding antigens.[3,4] Among the variety of immunoassays, the fluorescent immunoassay stands out as being one of the most widely used and most sensitive methods.[5,6]

The development of nanoscience and nanotechnology has brought great opportunities for immunoassays.[7] Nanoparticles (NPs), at least one dimension less than 100 nm, usually possess unique physical and chemical properties.[8] In addition, the cost of preparation of NPs is low, and they are easy to store and treat, facile to biofunctionalize, and are stable against denaturing. These advantages make them promising in the fabrication of immunosensors.[9] Recently, Yan and co-workers reported that Fe_3O_4 magnetic NPs, usually thought to be chemically and biologically inert, could catalyze the oxidation of typical organic substrates in the presence of H_2O_2.[10] After this pioneering work, a series of nanomaterials, such as $CoFe_2O_4$ NPs,[11] Co_3O_4 NPs,[12] CeO_2 NPs,[13] noble metal NPs,[14–16] and carbon-based nanomaterials,[17–19] have also been found to possess similar enzyme-like activity in aqueous media. Bioassays based on these smart materials have attracted tremendous interest, and are currently under intensive investigation, and this has been summarized in a recent review.[20] It is worth noticing that most of the reported bioassays have been focused on colorimetric analysis and for many of these nanomaterials, oxidizing agents (*e.g.* H_2O_2) or acid pH were needed to facilitate the oxidation of organic substrates,[21] which may limit their applications under physiological conditions. Therefore, it is still of great interest to exploit new applications of these smart materials and to develop new labels which can oxidize a substrate at neutral pH without H_2O_2.

CuS NPs, one of the most important metal chalcogenide semiconductors, are currently under intensive investigation due to their special electronic and optical properties. They have been widely applied in catalysis,[21,22] optical limiting,[23] photovoltaics[24] and biosensors.[25] In particular, their properties could be tuned by adjusting the structure, morphology, stoichiometric composition and valence state.[26] Up to now, several highly sensitive bioassays based on CuS NPs have been reported. For example, Zhang's group reported that CuS NPs were used for the ultrasensitive flow injection chemiluminescence detection of DNA hybridization.[27] Jan's group developed a sensitive electrochemical immunoassay based on the stripping voltammetric signals of Cu^{2+} dissolved from CuS NPs.[28] In our work, it was found that in the presence of CuS NPs, the non-fluorescent substrate *o*-phenylenediamine (OPD) could be oxidized into the stable fluorescent product 2,3-diamiophenazine (OPDox) at physiological pH. The fluorescent emission maximum of OPDox was at 558 nm. Throughout the

[a]*State Key Laboratory of Analytical Chemistry for Life Science, School of Chemistry and Chemical Engineering, Nanjing University, Nanjing 210093, P. R. China. E-mail: jianglp@nju.edu.cn; Fax: +86 2583597204; Tel: +86 25 83597204*

[b]*School of Chemistry and Chemical Engineering, Ningxia University, Yinchuan, 750021, P.R.China*

† Electronic supplementary information (ESI) available. See DOI: 10.1039/c3an01987j

reaction, no other oxidizing agents (*e.g.* H_2O_2) were needed and it could be deduced that CuS NPs acted as the oxidant in this reaction. The absence of other oxidizing agents avoided the negative response resulting from them, such as the instability coming from H_2O_2.[29] In addition, physiological pH reduced the possibility of protein denaturation, which was beneficial to the bioassay. This novel activity in aqueous media helped to widen the biochemical applications of CuS NPs.

OPD is a typical horseradish peroxidase (HRP) substrate. Colorless OPD can be oxidized into yellow OPDox and has been widely used for colorimetric and electrochemical immunoassays.[30,31] Apart from the colorimetric and electrochemical signals, OPDox also exhibits a stable fluorescent signal and could be used for highly-sensitive fluorescent analysis.[32] In our work, OPD was used for the first time as a substrate for a fluorescent immunoassay.

Herein, we used CuS NPs to label signal antibodies (Ab_2) and designed a highly sensitive immunoassay using MWCNTs to immobilize capture antibodies (Ab_1) (Scheme 1). In the presence of CuS NPs, OPD could be oxidized into the fluorescent product OPDox at physiological pH without any other oxidizing agent. The relatively mild oxidation conditions made the immunoassay robust, reliable and facile. The fluorescent intensity of OPDox at 558 nm was recorded to reflect the level of the corresponding antigen. This novel sandwich-type immunoassay was developed for the highly sensitive fluorescent detection of human prostate cancer biomarker, prostate specific antigen (PSA). The results showed that this immunoassay had excellent applicability for PSA detection. The proposed fluorescent immunosensor also offers an alternative strategy for the detection of other proteins and DNA.

Experimental

Materials and reagents

Cupric nitrate [$Cu(NO_3)_2 \cdot 3H_2O$] and bovine serum albumin (BSA) were obtained from Shanghai Reagent Company (Shanghai, China). Sodium sulfide ($Na_2S \cdot 9H_2O$), mercaptoacetic acid and *o*-phenylenediamine (OPD) were obtained from Sinopharm Chemical Reagent Co., Ltd. 1-Ethyl-3-(3-dimethylaminopropyl) carbodiimide hydrochloride (EDC), *N*-hydroxysuccinimide (NHS), Tween-20 and poly(diallyldimethylammonium chloride) (PDDA, 20 wt% in water, MW = 200 000–350 000) were obtained from Sigma-Aldrich. Multi-walled carbon nanotubes (MWCNTs, CVD method, purity > 95%, diameter 40–60 nm, length 5–15 μm) were from Shenzhen Nanotech Port Co., Ltd. Human PSA, McAb to PSA (Coating) (used as Ab_1) and McAb to PSA (Lable) (used as Ab_2) were purchased from Shanghai Linc-bio Science Co., Ltd (Shanghai, China). Indium tin oxide (ITO) coated glass slides (ITO coating 30 ± 5 nm, sheet resistance ≤ 10 Ω per square) were purchased from Nanjing Zhongjingkeyi Technology Co., Ltd (Nanjing, China). Phosphate buffer saline (PBS) of different pH values were prepared by mixing a stock solution of NaH_2PO_4 and Na_2HPO_4, and then adjusting the pH with 0.1 M NaOH and H_3PO_4. The wash buffer (PBST) was 10 mM, pH 7.4 PBS containing 0.05% Tween-20. All the reagents were of analytical grade and were used without further purification. Deionized and doubly distilled (DI) water was used throughout. The clinical serum samples were from Nanjing Gulou Hospital.

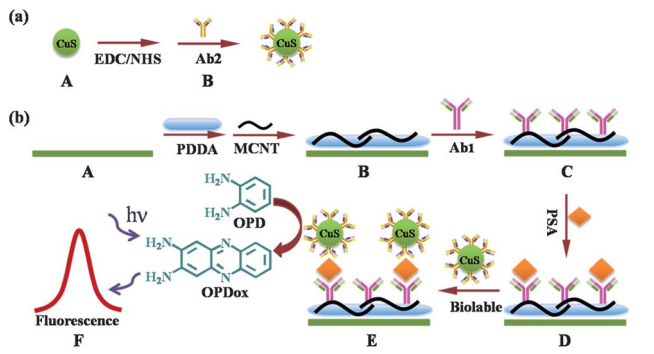

Scheme 1 (a) Schematic illustration of the fabrication of CuS–Ab_2 bioconjugate. (A) CuS NP. (B) CuS–Ab_2 bioconjugate. (b) Fabrication process of sandwich-type immunosensor for fluorescence detection of PSA. (A) ITO slice. (B) MWCNT/PDDA coated on ITO slice. (C) Immobilization of Ab_1. (D) Combination of target PSA. (E) CuS–Ab_2 bioconjugate captured by secondary immunoreaction. (F) PSA detection by fluorescence spectroscopy.

Characterization

The morphologies were observed by scanning electron microscopy, SEM (LEO153VP) and high-resolution transmission electron microscopy, HRTEM (JEOL JEM-200CX). Fourier transform infrared (FTIR) spectra were recorded with a Bruker model Vector 22 Fourier transform spectrometer using KBr pressed disks. X-ray powder diffraction (XRD) patterns were obtained with a Philips X'Pert X-ray diffractometer. X-ray photoelectron spectroscopic (XPS) measurements were carried out with an ESCALAB MK II X-ray photoelectron spectrometer. UV-Visible spectra were recorded on a UV-3600 spectrophotometer (Shimadzu). Fluorescence spectra were recorded on a RF-5301 PC spectrofluorophotometer (Shimadzu). Zeta potentials were measured with a PALS Zeta Potential Analyzer Ver. 3.43 (Brookhaven Instruments Corp.). Electrochemical impedance spectra were performed on an Auto-lab PGSTAT30 (Eco Chemie, B.V., Utrecht, The Netherlands) over a frequency range of 0.1–1.0 × 10^4 Hz in KCl solution (1.0 M) containing $K_3[Fe(CN)_6]$/$K_4[Fe(CN)_6]$ (10 mM, 1 : 1) mixture as a redox probe with an amplitude of 5 mV. All the measurements mentioned above were performed at room temperature.

Preparation of water soluble CuS NPs

CuS NPs were prepared according to the literature with some modification.[33] Briefly, 15 μL of mercaptoacetic acid was added to 50 mL of 2 mM $Cu(NO_3)_2$ solution. Then the pH of the solution was adjusted to 9.0 with 0.5 M NaOH aqueous solution. After bubbling with N_2 for 30 min, 5 mM Na_2S solution was added dropwise into the mixture to keep the molar ratio of Na_2S to $Cu(NO_3)_2$ at approximately 2.5. The reaction was carried out for 24 h under N_2 bubbling, and a dark green colloid was formed gradually. The product was washed with

ethanol and DI water several times to remove the residual ions and surfactant. Finally it was dispersed in water to form the CuS suspension.

Fabrication of CuS–Ab_2 probes

1 mL of the CuS suspension (0.5 mg mL^{-1}) was centrifuged and the supernatant solution was removed, followed by the addition of EDC (100 μL, 20 mg mL^{-1}) and NHS solution (100 μL, 10 mg mL^{-1}) to activate the carboxylic groups on the surface of the CuS NPs. After centrifugation and removal of the supernatant solution, 2 mL of Ab_2 (McAb to PSA, Lable) solution (0.1 mg mL^{-1}) was added. After being shaken gently overnight at 4 °C, the mixture was centrifuged and washed with PBST. The obtained bioconjugates were further washed with PBS three times and resuspended in 2 mL of PBS (10 mM, pH 7.4), then stored at 4 °C for subsequent use.

Fabrication of immunosensor

The fluorescent immunosensor was fabricated on an ITO slice. Prior to use, the ITO slice with an area of 5 × 15 mm was sonicated in acetone, ethanol and water for 15 min, respectively, then dried naturally at room temperature. After immersion into a solution of 1 : 1 (v/v) ethanol–NaOH (1 M) for 15 min, the ITO slice was rinsed with water, followed by immersion in PDDA (0.2%, in 0.1 M NaCl solution) for 30 min to modify the layer of PDDA. Then, 50 μL of 0.5 mg mL^{-1} carboxylic-functionalized MWCNTs[34] was dropped onto the substrate and dried naturally at room temperature. After that, 100 μL of an aqueous solution of 20 mg mL^{-1} EDC and 10 mg mL^{-1} NHS was added to activate the carboxylic groups on the surface of the MWCNTs for 30 min. After washing with PBST and PBS, the substrate was incubated with 100 μL of 30 μg mL^{-1} Ab_1 (McAb to PSA, coating) solution overnight at 4 °C. Next, the substrate was rinsed with PBST to remove the physically adsorbed Ab_1 and was then treated with 1 mL of 1% BSA solution containing 0.05% Tween to block any possible remaining active sites and to minimize non-specific adsorption during the immunoassay.

Immunoreaction and measurement procedure

For the immunoassay, the modified substrate was firstly incubated with 50 μL of target PSA or serum samples containing different concentrations of PSA for 50 min at 37 °C (the optimal conditions for immunoreactions), followed by washing three times with PBST. After that, the substrate was incubated with 50 μL of 75 μg mL^{-1} CuS–Ab_2 bioconjugates for 50 min at 37 °C and then washed thoroughly with PBST to remove non-specifically bonded conjugates. Then, the prepared substrate was incubated with 1 mL of 0.1 M PBS (pH 7.4) containing 2.0 mM OPD for 60 min at 40 °C in a sealed environment. Finally, the fluorescence emission spectra of the resulting solutions were recorded using a spectrofluorophotometer with an excitation wavelength of 392 nm for quantitative measurement of PSA.

Results and discussion

Preparation of CuS–Ab_2 probes

CuS NPs were prepared using mercaptoacetic acid as the stabilizer.[34] The CuS NPs were functionalized with carboxyl groups (see the FTIR spectrum in Fig. S1, ESI†). They had a relatively uniform morphology with an average diameter of about 10 nm (see the HRTEM image in Fig. S2, ESI†). When the prepared CuS NPs were dispersed in water, an homogeneous dark green suspension was formed and no sediment was observed even after 24 h (Fig. S3, ESI†), showing that the CuS NPs exhibited good stability and dispersibility in water. The as-prepared CuS NPs were characterized by XRD and XPS. All the diffraction peaks in the XRD pattern (Fig. S4, ESI†) could be well indexed to the hexagonal phase of CuS (JCPDS no. 06-0464). And no other diffraction peaks from impurities were observed, suggesting a high purity of the as-prepared CuS NPs. XPS was used to provide detailed information about the surface electronic state and the composition of the CuS NPs (Fig. S5, ESI†). The survey (full range) XPS spectrum (Fig. S5A†) showed the copper and sulfur peaks. A high-resolution spectrum of Cu 2p is presented in Fig. S5B.† The binding energies of 932.8 eV and 952.7 eV matched well with the Cu 2p3/2 and Cu 2p1/2 peaks of Cu^{2+} in CuS.[35,36] Moreover, a weak shake-up satellite peak at 943.2 eV was observed, indicating the presence of the paramagnetic chemical state of Cu^{2+}.[37,38] Furthermore, symmetrical shapes of the two Cu 2p XPS peaks also implied the presence of pure CuS.[39] The binding energy of S 2p appeared at 162.2 eV (Fig. S5C†), which is a typical value for metal sulfides.[40]

The antibodies of PSA (Ab_2) were conjugated to CuS NPs through an amidation reaction between the carboxyl groups on the NPs and the amine groups on the antibodies, as was shown in Scheme 1a. Before this, the carboxyl groups on the CuS NPs were first activated by EDC and NHS. As shown in Fig. 1, UV-Vis absorption spectrophotometry was used to characterize the CuS–Ab_2 bioconjugates. Compared with the original CuS NPs (Fig. 1, curve b), the bioconjugates showed an obvious absorbance around 280 nm (Fig. 1, curve c), which came from the antibodies (Fig. 1, curve a). The results indicated that the CuS–Ab_2 probes were successfully fabricated.

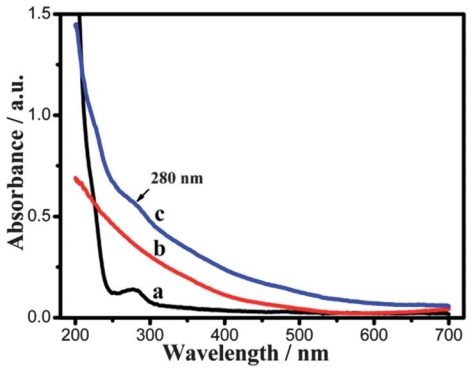

Fig. 1 UV-Vis absorption of (a) Ab_2, (b) CuS NPs, (c) CuS–Ab_2 bioconjugates.

Fabrication of the immunosensor

The carboxylated MWCNTs from chemical oxidation[34] (see the FTIR spectrum in Fig. S6, ESI†) were used as biosensing platforms for the immobilization of proteins. The carboxylated MWCNTs were negatively charged, with a zeta potential of −31.2 mV. In order to anchor the MWCNTs onto the ITO slice, positively charged PDDA (with a zeta potential of +40.5 mV) was used as the bridge. At first, the ITO slice was modified with a layer of PDDA *via* ionic reaction between PDDA and hydroxyl groups (–OH) on the ITO slice surface.[41] PDDA is a quaternary ammonium polyelectrolyte and is easily protonated. Then, through electrostatic adsorption with PDDA, the MWCNTs could be fixed on the ITO slice.

Because of the carboxyl groups on the MWCNTs, Ab_1 could be bound to the MWCNTs by a amidation reaction between the carboxyl groups and amine groups. The MWCNTs showed good biocompatibility and could make conjugated biomolecules with high stability and bioactivity.[42,43] Moreover, the MWCNTs provided an extremely large surface area for biomolecular conjugation, resulting in subsequent signal amplification and opening up the possibility of sensitivity improvement.[44] SEM was employed to characterize the MWCNTs and the Ab_1-immobilized MWCNTs on the ITO slice (Fig. 2). As shown in Fig. 2A, a layer of MWCNTs was assembled on the ITO slice, and the average diameter of the MWCNTs was 49 nm. After the immobilization of Ab_1, the average diameter of the MWCNTs increased to 60 nm and the surface of the MWCNTs became rough (Fig. 2B). This indicated that Ab_1 had been successfully trapped on the surface of the MWCNTs and the thickness of protein shell was about 11 nm.

Electrochemical impedance spectroscopy (EIS) was employed to characterize the fabrication process. Impedance spectra are composed of a semicircular portion at higher frequencies and a linear portion at lower frequencies. The semicircular portion corresponds to an electron-transfer-limited process, and the semicircle diameter is related to electron-transfer resistance (R_{et}). The linear portion corresponds to the diffusion process. Fig. 3 shows the Nyquist diagrams of EIS for bare ITO, PDDA/ITO, MWCNTs/PDDA/ITO and Ab_1/MWCNTs/PDDA/ITO, respectively. It was clear that the R_{et} value of bare ITO was lowest. After being modified with MWCNTs, ITO had a lower R_{et} value than that just modified with PDDA, because MWCNTs possessed excellent electrical conductivity, while PDDA did not. Then, after the immobilization of non-conductive Ab_1, the R_{et} value increased greatly which coincided with the fact that a layer of protein produced a barrier for electron transfer.

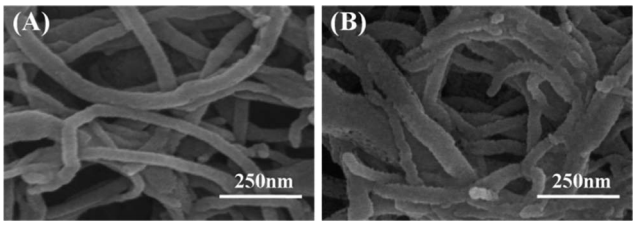

Fig. 2 SEM images of (A) MWCNTs coated on PDDA/ITO substrate, (B) immobilization of Ab_1 on MWCNTs.

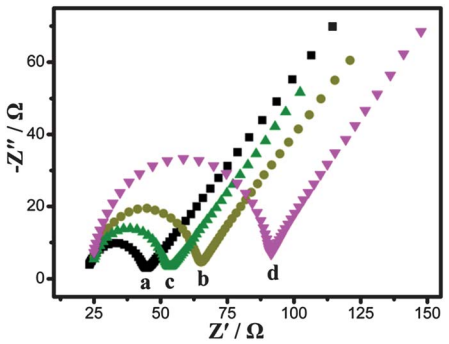

Fig. 3 Nyquist diagrams of EIS for (a) bare ITO, (b) PDDA/ITO, (c) MWCNTs/PDDA/ITO, (d) Ab_1/MWCNTs/PDDA/ITO, respectively, in KCl solution (1.0 M) containing $K_3[Fe(CN)_6]/K_4[Fe(CN)_6]$ mixture (10 mM, 1 : 1).

Fluorescence immunoassay using CuS–Ab_2 probes

In the presence of CuS NPs, the non-fluorescent substrate OPD could be oxidized into the fluorescent product OPDox, which had a maximal fluorescent emission at 558 nm (Fig. S7, ESI†). Throughout the reaction, no other oxidizing agents (*e.g.* H_2O_2) were needed and it could be deduced that the CuS NPs acted as the oxidant in the reaction. The labeling process of CuS to antibodies did not lead to a significant loss of its activity (Fig. S7C, ESI†). CuS NPs worked efficiently at physiological pH (Fig. S8A, ESI†) and maintained their activity over a wide range of temperatures (Fig. S8B, ESI†). At pH 7.4 and 40 °C, the obtained fluorescent intensity at 558 nm reached its maximum within 1 h and remained stable even after 24 h, which indicated that OPDox could provide very stable fluorescent signals. The immunoassay is outlined in Scheme 1b. CuS–Ab_2 probes were captured onto the immunosensor by means of a specific immunoreaction. The fluorescent intensity at 558 nm changed as the level of the corresponding antigen changed. Thus, the concentration of the target antigen could be detected by the sensitive fluorescent spectrometry. The relatively mild oxidation conditions made the immunoassay robust, reliable and facile.

Analytical performance

The change of the fluorescent intensity at 558 nm was investigated under different experimental conditions, including the concentration of Ab_1, incubation temperature, incubation time and the concentration of CuS–Ab_2 probes (Fig. 4). As a result, Ab_1 concentration of 30 μg mL^{-1}, incubation time of 50 min at 37 °C and CuS–Ab_2 concentration of 75 μg mL^{-1} were selected as the optimal immunoreaction conditions.

Under the optimized conditions, the fluorescent intensity at 558 nm increased as the concentration of the target PSA increased (Fig. 5A). The calibration plots showed a good linear relationship between the fluorescent intensity and the logarithm of the target antigen concentration[45] in the range from 0.0005 to 50 ng mL^{-1}. The linear regression equation was F/a.u.

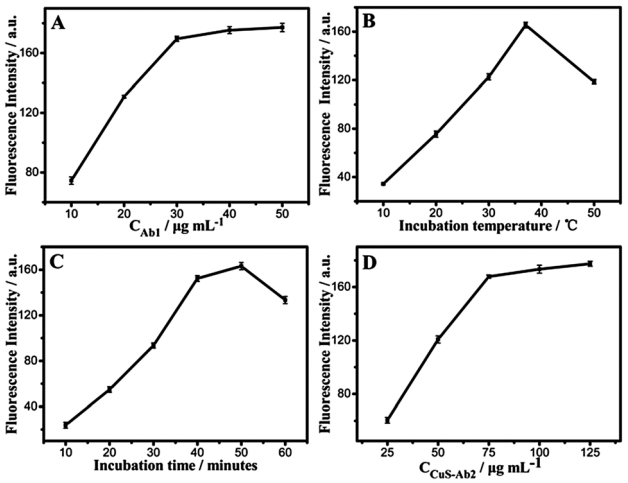

Fig. 4 Effects of (A) the concentration of Ab_1, (B) incubation temperature, (C) incubation time and (D) the concentration of CuS–Ab_2 probes in the immunoassay with an antigen concentration of 0.1 ng mL^{-1}.

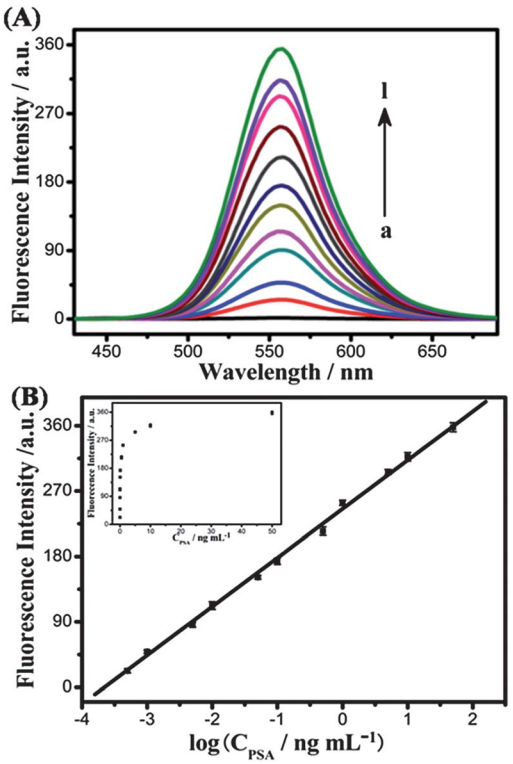

Fig. 5 (A) Fluorescence response of immunoassays with target PSA concentration of 0, 0.0005, 0.001, 0.005, 0.01, 0.05, 0.1, 0.5, 1, 5, 10, 50 ng mL^{-1} (curve a-l, respectively). (B) The resulting calibration curve of PSA plotted on a semi-log scale.

= 244.5 + 62.75 log(C_{PSA}/ng mL^{-1}) with a linear regression coefficient of 0.9982 (Fig. 5B). The detection limit ($S/N = 3$) was estimated to be 0.1 pg mL^{-1}. These results showed that compared with other methods for the determination of PSA, the proposed immunoassay was able to sensitively detect PSA over a relatively wider concentration range with a lower detection limit (as shown in Table S1, ESI†).[46–49] The low detection limit could be ascribed to the excellent activity of the CuS NPs, the good biocompatibility of the MWCNTs, and the large surface area of the MWCNTs for antibodies conjugation, which amplified the fluorescent signals and improved the sensitivity.

Specificity, reproducibility and stability of the immunosensor

The specificity plays a very important role in analyzing biological samples.[50] Other proteins, such as carcinoembryonic antigen (CEA), human interlekin-6 (IL-6), alpha fetoprotein (AFP) and immunoglobulin G (IgG), were used as interferents to evaluate the specificity of the proposed immunosensor. The fluorescent signals of 1.0 ng mL^{-1} PSA were compared with those obtained in the presence of 10 ng mL^{-1} of interfering substance (Table 1). The ratios of the fluorescence intensity for PSA alone and a mixture containing each interfering substance were 0.95, 1.05, 1.02, 0.97, respectively. These results indicated that the proposed immunosensor had high specificity.

The reproducibility of the proposed immunoassay was estimated by the relative standard deviations (RSD) of intra- and inter-assays. The intra-assay precision was determined by detecting three samples containing 0.01, 0.1, and 1 ng mL^{-1} PSA, respectively. Each sample was measured five times using five immunosensors prepared in parallel. The RSD values for the intra-assay were 5.34%, 4.31%, and 3.72%, respectively. The inter-assay RSD values were 2.89%, 2.04%, and 3.66% and were obtained by detecting each of the three samples five times using five separate sensors. The results showed that the proposed immunoassay was of satisfactory precision and reproducibility.

In addition, when the immunosensor was stored at 4 °C for 10, 20 and 30 days, 93%, 88% and 82% of the initial fluorescent response remained, respectively. The results indicated that the stability of the immunosensor was acceptable. The slight decrease of the signals might have something to do with deactivation and exfoliation of the immobilized antibodies.

Clinical applications in human serum

The feasibility of the immunoassay in comparison with the traditional ELISA method for clinical applications was investigated by analysing several real samples. Table 2 shows the relationship between the results obtained using the fluorescence immunoassay and those obtained with the ELISA method. No significant difference was observed, which

Table 1 Possible interferents tested with the proposed immunosensor

Possible interference	Fluorescence ratio[a]
Carcinoembryonic antigen (CEA)	0.95
Human interlekin-6 (IL-6)	1.05
Alpha fetoprotein (AFP)	1.02
Immunoglobulin G (IgG)	0.97

[a] Ratio of fluorescence intensity for 1.0 ng mL^{-1} PSA alone and a mixture containing 10 ng mL^{-1} interfering substance and 1.0 ng mL^{-1} PSA.

Table 2 Assay results of clinical serum samples using the proposed and ELISA methods

Serum samples	Proposed method[a] (ng mL^{-1})	ELISA[b] (ng mL^{-1})	Relative deviation (%)
1	5.062	5.000	1.24
2	1.500	1.590	−5.66
3	0.6702	0.6985	−4.05
4	0.1330	0.1260	5.57
5	0.0560	0.0570	−1.68
6	0.0254	0.0260	−2.23

[a] The average value of five successive determinations. [b] Given by the Affiliated Drum Tower Hospital of Nanjing University Medical School.

suggested that the proposed immunoassay could be applied in the clinical determination of PSA levels in human plasma.

Conclusions

In summary, a novel sensitive fluorescent immunoassay based on CuS NPs was successfully developed. In the presence of CuS NPs, the non-fluorescent substrate OPD could be oxidized into the very stable fluorescent product OPDox at physiological pH without any other oxidizing agent (*e.g.* H_2O_2). The relatively mild oxidation conditions made the immunoassay robust, reliable and facile. The proposed immunoassay exhibited high specificity, satisfactory reproducibility, acceptable stability and good accuracy for the detection of PSA. The method described here opens a new approach for the highly sensitive determination of other biomarkers, and is promising for point-of-care application for accurate clinical disease diagnosis.

Acknowledgements

We greatly appreciate the support from the National Natural Science Foundation of China (21121091, 21075061, 21265014) and the Program for New Century Excellent Talents in University (NCET-12-0256).

Notes and references

1 V. Gubala, L. F. Harris, A. J. Ricco, M. X. Tan and D. E. Williams, *Anal. Chem.*, 2012, **84**, 487–515.
2 J. A. Ludwig and J. N. Weinstein, *Nat. Rev. Cancer*, 2005, **5**, 845–856.
3 T. Li, E. J. Jo and M. G. Kim, *Chem. Commun.*, 2012, **48**, 2304–2306.
4 B. S. Munge, A. L. Coffey, J. M. Doucette, B. K. Somba, R. V. Patel, J. S. Gutkind and J. F. Rusling, *Angew. Chem., Int. Ed.*, 2011, **50**, 7915–7918.
5 D. A. Giljohann and C. A. Mirkin, *Nature*, 2009, **462**, 461–464.
6 L. Zhou, F. Ding, H. Chen, W. Ding, W. Zhang and S. Y. Chou, *Anal. Chem.*, 2012, **84**, 4489–4495.
7 Y. E. Choi, J. W. Kwak and J. W. Park, *Sensors*, 2010, **10**, 428–455.
8 C. Burda, X. B. Chen, R. Narayanan and M. A. El-Sayed, *Chem. Rev.*, 2005, **105**, 1025–1102.
9 M. Perfézou, A. Turner and A. Merkoçi, *Chem. Soc. Rev.*, 2012, **41**, 2606–2622.
10 L. Gao, J. Zhuang, L. Nie, J. Zhang, Y. Zhang, N. Gu, T. Wang, J. Feng, D. Yang, S. Perrett and X. Yan, *Nat. Nanotechnol.*, 2007, **2**, 577–583.
11 X. Zhang, S. He, Z. Chen and Y. Huang, *J. Agric. Food Chem.*, 2013, **61**, 840–847.
12 J. Xie and Y. Huang, *Anal. Methods*, 2011, **3**, 1149–1155.
13 A. Asati, S. Santra, C. Kaittanis, S. Nath and J. M. Perez, *Angew. Chem., Int. Ed.*, 2009, **48**, 2308–2312.
14 W. He, Y. Liu, J. Yuan, J. J. Yin, X. Wu, X. Hu, K. Zhang, J. Liu, C. Chen, Y. Ji and Y. Guo, *Biomaterials*, 2011, **32**, 1139–1147.
15 Y. Jv, B. Li and R. Cao, *Chem. Commun.*, 2010, **46**, 8017–8019.
16 K. Zhang, X. Hu, J. Liu, J. J. Yin, S. Hou, T. Wen, W. He, Y. Ji, Y. Guo, Q. Wang and X. Wu, *Langmuir*, 2011, **27**, 2796–2803.
17 Y. J. Song, X. H. Wang, C. Zhao, K. G. Qu, J. S. Ren and X. G. Qu, *Chem.–Eur. J.*, 2010, **16**, 3617–3621.
18 W. Shi, Q. Wang, Y. Long, Z. Cheng, S. Chen, H. Zheng and Y. Huang, *Chem. Commun.*, 2011, **47**, 6695–6697.
19 Y. Song, K. Qu, C. Zhao, J. Ren and X. Qu, *Adv. Mater.*, 2010, **22**, 2206–2210.
20 J. Xie, X. Zhang, H. Wang, H. Zheng and Y. Huang, *TrAC, Trends Anal. Chem.*, 2012, **39**, 114–129.
21 Y. Song, W. Wei and X. Qu, *Adv. Mater.*, 2011, **23**, 4215–4236.
22 W. He, H. Jia, X. Li, Y. Lei, J. Li, H. Zhao, L. Mi, L. Zhang and Z. Zheng, *Nanoscale*, 2012, **4**, 3501–3506.
23 J. Zhang, J. Yu, Y. Zhang, Q. Li and J. R. Gong, *Nano Lett.*, 2011, **11**, 4774–4779.
24 J. N. Gao, Q. S. Li, H. B. Zhao, L. S. Li, C. L. Liu, Q. H. Gong and L. M. Qi, *Chem. Mater.*, 2008, **20**, 6263–6269.
25 A. B. F. Martinson, J. W. Elam and M. J. Pellin, *Appl. Phys. Lett.*, 2009, **94**, 123107.
26 J. Liu and D. Xue, *J. Mater. Chem.*, 2011, **21**, 223–228.
27 P. Leidinger, R. Popescu, D. Gerthsen, H. Lünsdorf and C. Feldmann, *Nanoscale*, 2011, **3**, 2544–2551.
28 S. S. Zhang, H. Zhong and C. F. Ding, *Anal. Chem.*, 2008, **80**, 7206–7212.
29 G. D. Liu, J. Wang, J. Kim and M. R. Jan, *Anal. Chem.*, 2004, **76**, 7126–7130.
30 A. Asati, C. Kaittanis, S. Santra and J. M. Perez, *Anal. Chem.*, 2011, **83**, 2547–2553.
31 A. Ambrosi, M. T. Castaneda, A. J. Killard, M. R. Smyth, S. Alegret and A. Merkocüi, *Anal. Chem.*, 2007, **79**, 5232–5240.

32 R. Cui, H. Huang, Z. Yin, D. Gao and J. J. Zhu, *Biosens. Bioelectron.*, 2008, **23**, 1666–1673.
33 X. Yang and E. Wang, *Anal. Chem.*, 2011, **83**, 5005–5011.
34 S. Bi, H. Zhou and S. Zhang, *Chem. Sci.*, 2010, **1**, 681–687.
35 V. Datsyuk, M. Kalyva, K. Papagelis, J. Parthenios, D. Tasis, A. Siokou, I. Kallitsis and C. Galiotis, *Carbon*, 2008, **46**, 833–840.
36 J. Zhang, J. Yu, Y. Zhang, Q. Li and J. R. Gong, *Nano Lett.*, 2011, **11**, 4774–4779.
37 L. Zhang, T. Jiang, S. Li, Y. Lu, L. Wang, X. Zhang, D. Wang and T. Xie, *Dalton Trans.*, 2013, **42**, 12998–13003.
38 Y. Zhang, J. Tian, H. Li, L. Wang, X. Qin, A. M. Asiri, A. O. AlYoubi and X. Sun, *Langmuir*, 2012, **28**, 12893–12900.
39 L. Mikyyung and K. J. Yong, *Nanotechnology*, 2012, **23**, 194014–194017.
40 J. Yu, J. Zhang and S. Liu, *J. Phys. Chem. C*, 2010, **114**, 13642–13649.
41 V. I. Nefedov, Y. V. Salyn, P. M. Solozhenkin and G. Y. Pulatov, *Surf. Interface Anal.*, 1980, **2**, 170–172.
42 R. J. Cui, H. C. Pan, J. J. Zhu and H. Y. Chen, *Anal. Chem.*, 2007, **79**, 8494–8501.
43 R. Cui, C. Liu, J. Shen, D. Gao, J. J. Zhu and H. Y. Chen, *Adv. Funct. Mater.*, 2008, **18**, 2197–2204.
44 Q. Zhang, B. Zhao, J. Yan, S. Song, R. Min and C. Fan, *Anal. Chem.*, 2011, **83**, 9191–9196.
45 J. Peng, L. N. Feng, K. Zhang, X. H. Li, L. P. Jiang and J. J. Zhu, *Chem.–Eur. J.*, 2012, **18**, 5261–5268.
46 A. M. Ward, J. W. F. Catto and F. C. Hamdy, *Ann. Clin. Biochem.*, 2001, **38**, 633–651.
47 R. Akter, M. A. Rahman and C. K. Rhee, *Anal. Chem.*, 2012, **84**, 6407–6415.
48 Z. Gao, M. Xu, L. Hou, G. Chen and D. Tang, *Anal. Chem.*, 2013, **85**, 6945–6952.
49 F. Liu, Y. Zhang, S. Ge, J. Lu, J. Yu, X. Song and S. Liu, *Talanta*, 2012, **99**, 512–519.
50 M. Wang, L. Wang, G. Wang, X. Ji, Y. Bai, T. Li, S. Gong and J. Li, *Biosens. Bioelectron.*, 2004, **19**, 575–582.